CVI Journals.ASM.org

Herpes Simplex Virus 1 Suppresses the Function of Lung Dendritic Cells via Caveolin-1

Bing Wu,[a] Shuang Geng,[b] Yanmin Bi,[a] Hu Liu,[a] Yanxin Hu,[c] Xinqiang Li,[a] Yizhi Zhang,[a] Xiaoyu Zhou,[b] Guoxing Zheng,[d] Bin He,[d] Bin Wang[a,b]

State Key Laboratory for Agro-Biotechnology, College of Biological Science, China Agricultural University, Beijing, People's Republic of China[a]; Key Laboratory of Medical Molecular Virology of MOH and MOE, Fudan University Shanghai Medical College, Shanghai, People's Republic of China[b]; College of Veterinary Medicine, China Agricultural University, Beijing, People's Republic of China[c]; Department of Microbiology and Immunology, College of Medicine, University of Illinois, Chicago, Illinois, USA[d]

Caveolin-1 (Cav-1), the principal structural protein of caveolae, has been implicated as a regulator of virus-host interactions. Several viruses exploit caveolae to facilitate viral infections. However, the roles of Cav-1 in herpes simplex virus 1 (HSV-1) infection have not fully been elucidated. Here, we report that Cav-1 downregulates the expression of inducible nitric oxide synthase (iNOS) and the production of nitric oxide (NO) in dendritic cells (DCs) during HSV-1 infection. As a result, Cav-1 deficiency led to an accelerated elimination of virus and less lung pathological change following HSV-1 infection. This protection was dependent on iNOS and NO production in DCs. Adoptive transfer of DCs with Cav-1 knockdown was sufficient to confer the protection to wild-type (WT) mice. In addition, Cav-1 knockout (KO) (Cav-1$^{-/-}$) mice treated with an iNOS inhibitor exhibited significantly reduced survival compared to that of the nontreated controls. We found that Cav-1 colocalized with iNOS and HSV-1 in caveolae in HSV-1-infected DCs, suggesting their interaction. Taken together, our results identified Cav-1 as a novel regulator utilized by HSV-1 to evade the host antiviral response mediated by NO production. Therefore, Cav-1 might be a valuable target for therapeutic approaches against herpesvirus infections.

Herpes simplex virus 1 (HSV-1) is a double-stranded DNA (dsDNA) virus belonging to the *Alphaherpesvirus* family, which causes oral herpes, encephalitis, keratitis, neonatal herpes, and pneumonia disease, establishing latency in the neurons after acute infection of mucosal tissues (1–3). Notably, HSV-1 can be isolated from the respiratory tract of immunosuppressed patients and newborn infants, where it induces pneumonitis, resulting in remarkable morbidity and mortality (4). Recent studies have suggested that HSV-1-induced bronchopneumonitis is common in nonimmunocompromised persons who are undergoing continuous mechanical ventilation (5). Currently, the mechanisms of HSV-1-induced pneumonia and obstructive pulmonary disease are not fully understood, although intranasal (i.n.) infection with HSV-1 in mice can be used as a model to investigate these mechanisms (4, 6, 7). Such investigations might reveal a valuable therapeutic approach for HSV-1-induced pneumonia.

Innate defense cells and inflammatory factors serve as the first-line of host defense against viral infections. DCs can be recruited to the lungs and in the cornea of the eye, where they contribute to host defense (8, 9). Studies have shown that diphtheria toxin (DT)-induced depletion of DCs in CD11c-DTR mice (in which the DT receptor [DTR] is expressed under the control of the CD11c promoter) inhibited the migration of natural killer cells and neutrophils to locally infected cornea, resulting in severe pathology (10, 11). Moreover, involvement of the free radical nitric oxide (NO) has been indicated. This is a powerful vasodilator factor and cell signaling molecule, with a short half-life of 3 to ~4 s in the blood, and it is synthesized by nitric oxide synthase (NOS) in epithelial cells, macrophages, DCs, and other myeloid cells (12, 13). NOS has three isoenzymes: endothelial NOS (eNOS), neuronal NOS (nNOS), and inducible NOS (iNOS) (iNOS is induced by a single stimulus, like lipopolysaccharide [LPS] or gamma interferon [IFN-γ]). Induction of iNOS and NO production constitutes a critical component of the innate antiviral host response to HSV-1, influenza A virus, and other intracellular parasites (14–16) and is potent in clearing the invading pathogens. Early inhibition of NO by i.n. administration of aminoguanidine (AG) was found to increase HSV-1 infection in the eyes and lungs of mice (17). Conversely, pretreatment with an NO donor, sodium nitroprusside (SNP), decreased the titer of Sindbis virus (18). Despite the general importance of DCs and NO in antiviral responses, it is unknown whether this is applicable to HSV-1 infection in the lungs.

Caveolin-1 (Cav-1), a scaffolding protein found in most types of cells, is the major coating protein of caveolae (with 50- to 100-nm plasma membrane invaginations) (19, 20). A deficiency in Cav-1 leads to disruption of the caveolae structure. Although best known in lipid metabolism, roles for Cav-1 in the internalization of pathogens, signal transduction, host defenses, and suppression of inflammatory responses have also been indicated by numerous studies (20–22). Viral entry into cells occurs by clathrin, caveolae, or receptor-mediated pathways (23–25). However, recent studies revealed that simian virus 40 (SV40) enters cells via

Received 24 March 2015 **Returned for modification** 10 April 2015
Accepted 20 May 2015
Accepted manuscript posted online 27 May 2015
Citation Wu B, Geng S, Bi Y, Liu H, Hu Y, Li X, Zhang Y, Zhou X, Zheng G, He B, Wang B. 2015. Herpes simplex virus 1 suppresses the function of lung dendritic cells via caveolin-1. Clin Vaccine Immunol 22:883–895. doi:10.1128/CVI.00170-15.
Editor: H. F. Rosenberg
Address correspondence to Bin Wang, bwang3@fudan.edu.cn.

doi:10.1128/CVI.00170-15

an atypical caveolae-mediated endocytic pathway, forming a new compartment called a caveosome (26, 27). Amphotropic murine leukemia virus (A-MLV) also infects NIH 3T3 cells via Pit2 with the involvement of caveolae (28).

In addition, published work has suggested that Cav-1 facilitates viral replication *in vitro* and regulates inflammation *in vivo*. Cav-1 was observed to facilitate influenza A virus subtype H1N1 replication, while Cav-1 mutations or RNA interference (RNAi)-mediated Cav-1 knockdown decreased the virus titer in infected Madin-Darby canine kidney (MDCK) cells (29). By using the mutant Cav-1 protein, hepatitis B virus (HBV) was found to require intact Cav-1 to initiate a productive infection in HepaRG cells (30). In addition, Cav-1 has been implicated in cell signaling and inflammation (31). Reports show that caveolin-1 might downregulate iNOS/NO via a proteasome pathway and mediate the posttranscriptional regulation of iNOS (32, 33). Through the ability of Cav-1 to regulate NO, Cav-1$^{-/-}$ mice exhibited attenuation of lung injury and less edema formation in response to LPS (34). These observations suggested to us that Cav-1 might be involved in HSV-1 infection.

We hypothesized that Cav-1 might suppress host antiviral immunity during HSV-1 infection. In the present study, we used a murine model of HSV-1-induced pneumonia to demonstrate for the first time that Cav-1$^{-/-}$ mice are resistant to fatal HSV-1 infection and that the increased antiviral activity is due to increased expression of iNOS/NO in DC cells in Cav-1$^{-/-}$ mice. In addition, the protective effect of Cav-1 deficiency was largely abolished by iNOS inhibition in Cav-1$^{-/-}$ mice or by DC depletion in CD11c-DTR/Cav-1$^{-/-}$ mice. Furthermore, we observed that Cav-1 colocalized with iNOS and HSV-1 in caveolae in the virus-infected DCs. Thus, these findings indicate that HSV-1 exploits Cav-1 to downregulate the expression of iNOS in DCs. The corollary is that a deficiency in Cav-1 can restore antiviral immune responses, which has implications for the design of drugs against herpes infection.

MATERIALS AND METHODS

Ethics statement. The use of laboratory animals in our study was approved by the Beijing Association for Science and Technology (approval ID SYXK [Beijing] 2007-0023), and all animal procedures were conducted according to the guidelines of Beijing Laboratory Animal Welfare and Ethics of the Beijing Administration Committee of Laboratory Animals. All animal research was also carried out in accordance with the China Agricultural University Institutional Animal Care and Use Committee guidelines (ID: SKLAB-B-2010-003) and approved by the animal welfare committee of China Agricultural University.

Mice. Female C57BL/6 mice at 6 to 8 weeks of age were purchased from the Animal Institute of Chinese Medical Academy (Beijing, China). Cav-1$^{-/-}$ mice (stock Cav1^{tm1Mls}/J, C57BL/6 background) and CD11c-DTR-GFP mice (B6.FVB-Tg [Itgax-DTR/GFP] 57Lan/J) (GFP, green fluorescent protein) were purchased from the Jackson Laboratory (Bar Harbor, ME). NOS2 (iNOS) KO mice (B6, 129P2-NOS2^{tm1Lau}/J) were purchased from the China Institute of Laboratory Animal Sciences, Chinese Academy of Medical Sciences (CAMS), and Peking Union Medical College (PUMC).

Reagents. *S*-methylisothiourea sulfate (SMT), an iNOS inhibitor, and radioimmunoprecipitation assay (RIPA) lysis buffer were obtained from the Beyotime Institute of Biotechnology (Beijing, China). DAPI (4′,6-diamidino-2-phenylindole) and mitomycin C were obtained from Sigma (St. Louis, MO, USA). Rabbit polyclonal anti-iNOS antibody was obtained from Cell Signaling Technology (Danvers, MA, USA), goat anti-iNOS antibody was from Santa Cruz (Dallas, TX, USA), anti-glyceraldehyde-3-phosphate dehydrogenase (GAPDH) antibody was obtained from Ambion Life Technologies (Waltham, MA, USA), and anti-Cav-1 and anti-HSV-1 antibodies (Abs) were obtained from Abcam (Hong Kong, China). Goat anti-mouse IgG-horseradish peroxidase (HRP), goat anti-rabbit IgG-HRP, bovine anti-goat IgG-HRP, goat anti-rabbit-IgG-phycoerythrin/fluorescein isothiocyanate (PE/FITC), and bovine anti-goat IgG-FITC/PE antibodies were purchased from Santa Cruz Biotechnology. RNase-free DNase I was purchased from Promega (Madison, WI, USA). The DNA extraction kit and total RNA extraction kit were obtained from Omega (Norcross, GA, USA). ReverTra Ace and the SYBR green real-time PCR kit were obtained from Toyobo Life Science (Osaka, Japan).

Virus and cells. HSV-1 strain F was originally obtained from the National Institutes for Food and Drug Control (China) and was propagated in Vero cells. Virus was harvested by repeated freezing and thawing and concentrated by centrifugation at 18,000 × *g* for 2 h at 4°C before cell debris removal by centrifugation at 8,000 × *g* and 4°C. Virus stock was stored at −80°C. DC2.4 is a DC cell line from C57BL/6 mice. Cav-1 knockdown DC2.4 cells and Cav-1 overexpressing DC2.4 cells were generated as previously described (23). Vero cells and DC2.4 cell lines were maintained in Dulbecco's modified Eagle's medium (DMEM) supplemented with 10% heat-inactivated fetal bovine serum (FBS) and 1% penicillin-streptomycin at 37°C with 5% CO_2. CD11c$^+$ DCs were isolated from spleen with CD11c MicroBeads, according to the manufacturer's instructions (Miltenyi Biotech, Cologne, Germany). The efficiency of isolation was assessed by flow cytometry assay, as previously described (35).

Viral titers and HSV-1 infection. HSV-1 was titrated by the 50% tissue culture infectious dose ($TCID_{50}$) method in Vero cells. Monolayers of Vero cells were prepared at 80 to 90% density in a 96-well plate. Serial dilutions of HSV-1 (10^{-1} to 10^{-10}) were incubated in the wells until the appearance of cytopathic effects (CPE) (which include the ballooning of cells and multinucleated cell formation). The viral titer ($TCID_{50}$) was determined by the Reed-Muench method at day 4.

Age- and sex-matched mice were anesthetized by intraperitoneal (i.p.) injection with pentobarbital sodium at 50 mg/kg of body weight and i.n. inoculated with 3×10^{10} or 3×10^{9} $TCID_{50}$ of HSV-1 as required.

Tissue sampling and cell isolation. To obtain DCs, a bronchoalveolar lavage fluid (BALF) sample was collected in 1.5-ml aliquots of phosphate-buffered saline (PBS) from the right lobe of the lung with the left lobe ligated onto infusion lines, and PBS was infused and withdrawn five times. After centrifugation at 1,000 × *g* for 5 min, the supernatant was stored at −20°C for further testing. CD11c$^+$ DCs were isolated from lung cells with CD11c MicroBeads, as per the manufacturer's instructions. The left lobe of the lung was fixed in 4% paraformaldehyde for histological examination. To obtain pulmonary alveolar macrophages, BALF was collected in 2-ml aliquots of RPMI 1640 medium containing 1% penicillin-streptomycin solution. The medium was infused and withdrawn 6 to 8 times, and the cells were separated by the surface adhesion method. A single cell suspension from whole lung was prepared by homogenization in RPMI 1640 medium with 1% penicillin-streptomycin. Red blood cells were removed with red blood cell (RBC) buffer, and 12-well plates were seeded at 37°C with 5% CO_2 for 45 min. Cells suspended in medium were purified twice by attachment, and then the lung epithelial cells were collected for total DNA extraction.

Adoptive transfer. Mitomycin C-pretreated DC2.4 cells, DC2.4 with Cav-1 knockdown, and DC2.4 with Cav-1-overexpression were adoptively transferred intratracheally (i.t.) to the lungs of recipient mice. Twelve hours later, mice were challenged i.n. with 10 50% lethal doses (LD_{50}) of HSV-1. The survival of transferred carboxyfluorescein succinimidyl ester (CFSE)-labeled DC cells in lungs was detected by a fluorescence-activated cell sorter (FACS) at days 1 and 5 postinfection. The results showed that transferred DCs survived in lungs over the course of HSV-1 infection.

SMT treatment. Cav-1-deficient mice were treated with SMT (an iNOS inhibitor) by an i.p. injection (50 mg/kg) at 12 h prior to HSV-1

infection, followed by daily administration until 12 days postinfection (dpi).

***In vivo* CD11c$^+$ DC depletion with diphtheria toxin.** A transgene was designed to place a simian diphtheria toxin receptor (DTR) protein under the control of the CD11c promoter, and CD11c-DTR mice were generated (36). CD11c$^+$ DCs in CD11c-DTR mice were depleted with diphtheria toxin (DT) (Sigma). DT was prepared in a sterile solution of PBS with 0.5% lactose. Mice were given an i.p. injection of DT at 8 ng/g of body weight at 12 h prior to HSV-1 challenge and every 12 h after until 12 dpi. The efficiency of depletion was detected by flow cytometry.

mRNA expression profiling in infected lung cells. Total RNA was isolated with the total RNA extraction kit. cDNA was synthesized using the Toyobo ReverTra Ace and oligo(dT)$_{18}$ primers with 1 μg of RNA. Real-time PCR was performed by using an ABI 7900 real-time PCR system with a SYBR green real-time PCR master mix plus kit. Gene expression was normalized with the housekeeping gene GAPDH. The primers were: for COX-2, forward primer 5′-TGAGCAACTATTCCAAACCAGC-3′ and reverse primer 5′-GCACGTAGTCTTCGATCACTATC-3′; for eNOS, forward primer 5′-CAACGCTACCACGAGGACATT-3′ and reverse primer 5′-CTCCTGCAAAGAAAAGCTCTGG-3′; for suppressor of cytokine signaling 1 (SOCS-1), forward primer 5′-GTGGTTGTGGAGGGTGAGAT-3′ and reverse primer 5′-CCTGAGAGGTGGGATGAGG-3′; for interleukin 10 (IL-10), forward primer 5′-AGAAGCATGGCCCTGAAATCAAGG-3′ and reverse primer 5′-CTTGTAGACACCTTGGTCTTGGAG-3′; for IL-1β, forward primer 5′-CAACCAACAAGTGATATTCTCCATG-3′ and reverse primer 5′-GATCCACACTCTCCAGCTGCA-3′; for iNOS, forward primer 5′-TCGCTTTGCCACGGACGAGA-3′ and reverse primer 5′-TGGCCAGCTGCTTTTGCAGG-3′; for extracellular-signal-regulated kinase 1 (ERK1), forward primer 5′-GCGTTACATGTGGCAGCTTGA-3′ and reverse primer 5′-TGGAACCCCACCCCATTTT-3′; for IFN-β, forward primer 5′-AGCTCCAAGAAAGGACGAACAT-3′ and reverse primer 5′-GCCCTGTAGGTGAGGTTGATCT-3′; for CD40, forward primer 5′-GCCATCGTGGAGGTACTGTT-3′ and reverse primer 5′-CTGCGATGGTGTCTTTGCCT-3′; for programmed cell death ligand 1 (PD-L1), forward primer 5′-ATGCTGCCCTTCAGATCACAG-3′ and reverse primer 5′-TGGTTGATTTTGCGGTATGGG-3′; for GAPDH, forward primer 5′-GCACAGTCAAGGCCGAGAAT-3′ and reverse primer 5′-GCCTTCTCCATGGTGGTGAA-3′.

Viral load assay. Cell genomic DNA was extracted with a DNA extraction kit after infection of lungs or DC cells by HSV-1. The copy number of the polymerase (Pol) gene of HSV-1 was calculated by using a Pol-containing plasmid of known concentration as a standard. Real-time PCR was performed as described above. Gene-specific primers for Pol were designed, with forward primer 5′-GCTCGAGTGCGAAAAAACGTTC-3′ and reverse primer 5′-CGGGGCGCTCGGCTAAC-3′.

Western blot assay. After infection with HSV-1, DC2.4 cells or lung cells were lysed using RIPA lysis buffer with 100 U of proteinase inhibitor (Promega), protein was quantified with a bicinchoninic acid (BCA) assay kit (Pierce Biotechnology, Inc.), and the lysates were stored at −80°C. Approximately 30 μg of protein was loaded onto a 10% SDS-PAGE gel. After electrophoresis, proteins were transferred to polyvinylidene difluoride (PVDF) membranes (Millipore, Darmstadt, Germany) before the membranes were blocked with 5% bovine serum albumin (BSA) in PBS containing 0.05% Tween 20. The membranes were then incubated with antibodies for 2 h at room temperature at a suitable dilution, as recommended by the manufacturer (anti-Cav-1 antibody diluted at 1:1,000, anti-HSV-1 at 1:1,000, anti-β-actin at 1:10,000, and anti-GAPDH at 1:5,000) and then reacted with HRP-conjugated goat anti-mouse IgG, goat anti-rabbit IgG, or bovine anti-goat IgG (Santa Cruz Biotechnology) as secondary antibodies at a dilution of 1:5,000. The bound conjugates were detected with Millipore ECL reagents.

***In vitro* NO assay.** NO in serum, BALF, and cell culture supernatants was measured by the nitrate/nitrite colorimetric assay kit (lactate dehydrogenase [LDH] method; Cayman Chemical, MI, USA). Samples were centrifuged at 10,000 × *g* for 5 min, and the supernatants were collected for assay of the total NO products with PBS or DMEM as a control. Measurement of nitrate was performed according to the manufacturer's instructions. After incubation with Griess reagent R1/R2 for 10 min, absorbance at a wavelength of 540 nm was measured with a microplate spectrophotometer reader (Bio-Tek Instruments, Inc., Winooski, VT, USA). NO concentrations were calculated using a nitrate standard curve.

Confocal microscopy. DC cells were plated in chamber slides (Nunc, Waltham, MA, USA), infected with HSV-1, fixed with 4% paraformaldehyde for 10 min, and permeabilized with 0.1% Triton X-100 for 3 min. After incubation in blocking buffer, the cells were stained with anti-iNOS and anti-Cav-1 or anti-HSV-1 antibody (1:150 diluted) overnight at 4°C in a humidity chamber. After washing five times with PBS, the cells were then incubated with goat anti-rabbit IgG-PE/FITC or bovine anti-goat-FITC/PE for 1 h, stained with DAPI for 3 min, and then washed 5 times with PBS. Immunofluorescence was observed using a Nikon A1 or Nikon N-SIM confocal microscope and analyzed using the Nikon EZ-C1 3.00 FreeViewer software.

Co-IP assay. A coimmunoprecipitation (Co-IP) experiment was performed to detect the interaction of iNOS with caveolin-1. A Pierce classic magnetic IP and Co-IP kit (Thermo) were used. A total of 2×10^6 DC cells were seeded and infected with HSV-1 at a multiplicity of infection (MOI) of 5. At 24 and 48 h postinfection (hpi), Co-IP analysis was done according to the kit manufacturer's instructions. In brief, cells were harvested with ice-cold IP lysis/wash buffer. Cell debris was removed by centrifugation at ~13,000 × *g* for 10 min. One milligram of total protein in supernatant was transferred to a new tube, mixed with 5 μg of IP antibody (anti-Cav-1; Abcam), and left overnight at 4°C in a tube roller to form immune complexes. Pierce protein A/G magnetic beads were washed with IP lysis/wash buffer, added to the antigen sample-antibody mixture, and incubated at room temperature for 1 h with mixing. Next, beads were collected with a magnetic stand and washed twice with IP lysis/wash buffer and once with ultrapure water. Complex was eluted from the beads with lane marker sample buffer containing 50 nM dithiothreitol (DTT) as provided in the kit, and then the supernatant was immunoblotted.

Histopathology. Seven days after HSV-1 challenge, lung, brain, liver, kidney, heart, and spleen samples were collected from each group of mice and fixed in 4% paraformaldehyde. After paraffin embedding, the tissues were cut into 4- to 5 μm-thick sections. Antigen retrieval was accomplished by boiling the slides in 0.01 M citrate buffer (pH 6.0), followed by staining with hematoxylin and eosin (H&E). Immunohistochemistry of HSV-1 antigen in lung and brain sections was performed as previously described (37).

Statistical analysis. The results are presented as the mean ± standard error of the mean (SEM) from at least three independent experiments. Treatment groups were compared by Student's *t* test and nonparametric analysis of variance (ANOVA). Pairwise differences were analyzed by the two-sided Student's *t* test. For multigroup analysis, ANOVA was used. A P value of <0.05 was considered to be statistically significant. For survival curve analysis, a log rank (Mantel-Cox) test was performed, and a P value of <0.05 denoted a statistically significant difference.

RESULTS

Cav-1-deficient mice are more resistant to HSV-1 infection. To investigate the potential role of Cav-1 in the host defense upon infection, we initially infected wild-type (WT) C57BL/6 mice with different doses of HSV-1 (50 μl of 10^8, 10^9, and $10^{9.47}$ $TCID_{50}$ of HSV-1) via the i.n. route, and the survival of the animals was monitored. As shown in Fig. 1A, 50% of the mice died after infection with $10^{9.47}$ (3×10^9) $TCID_{50}$ of HSV-1, indicating that the $LD_{50}$of HSV-1 was 3×10^9 $TCID_{50}$ in mice with the C57BL/6 background. To assess the role of Cav-1 in resistance to infection, both WT and Cav-1$^{-/-}$ mice were challenged with a lethal dose (10 LD_{50}) of HSV-1, and the survival of the animals was monitored. During the first 8 days after challenge, Cav-1$^{-/-}$ mice had a

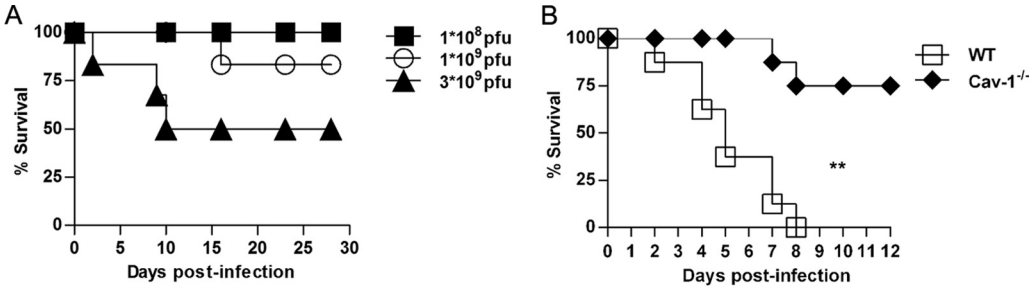

FIG 1 Cav-1-deficient mice are relatively resistant to HSV-1 infection. (A) Groups of WT C57BL/6 mice ($n = 6$) were challenged i.n. with HSV-1 at 1×10^8, 1×10^9, or 3×10^9 $TCID_{50}$, and the percent survival was observed until 30 dpi. (B) Groups of WT and Cav-$1^{-/-}$ mice ($n = 8$) were challenged with 10 LD_{50} of HSV-1 (3×10^{10} $TCID_{50}$). Survival is represented according to the Mantel-Cox log rank test. The data are representative of three individual experiments. **, $P < 0.01$.

higher survival rate than that of WT mice (75% in Cav-$1^{-/-}$ mice versus 0% in WT mice) (Fig. 1B), showing that Cav-$1^{-/-}$ mice are more resistant to HSV-1 infection.

Cav-1 deficiency correlates with reduced viral replication and lung pathology. Because virus replication and the consequent tissue damage are thought to contribute to the mortality of mice during viral infection, the influence of Cav-1 on both viral load and histopathology was investigated. We challenged WT and Cav-$1^{-/-}$ mice with 10 LD_{50} of HSV-1 via the i.n. route. On day 7 postinfection, we determined histology and viral replication in the lungs, brain, heart, liver, spleen, and kidneys. HSV-1 did not cause obvious tissue damage in most organs examined except the brain and lungs (Fig. 2A). There was no difference between Cav-$1^{+/+}$ and Cav-$1^{-/-}$ mice in the degree of damage in brain sections, indicating that less brain damage did not account for the greater resistance of the Cav-$1^{-/-}$ mice (Fig. 2A). However, the lungs from Cav-$1^{-/-}$ mice showed much less lung destruction than that of the WT mice, which had substantial cell infiltration edema, thickening of the alveolar wall, and alveolar septum capillary congestion (Fig. 2B). Despite the greater cell infiltration observed in the WT mouse lung sections, no major differences in total BALF cell counts were detectable between the two groups (data not shown). Histopathology scores were significantly lower in Cav-$1^{-/-}$ mice than those in WT mice (average score, 2.6 in Cav-$1^{-/-}$ mice and 3.8 in WT mice; Fig. 2C). When viral load in the organs was assessed by quantitative PCR (qPCR) at day 7 after HSV-1 infection, viral load was correlated with the histochemical results, being barely detected in the liver, spleen, and kidneys (Fig. 2D). The viral load was also remarkably less in Cav-$1^{-/-}$ lung cells and in BALF ($10^{1.67}$-fold lower), whereas no obvious difference in load was seen in the brain at 7 dpi (Fig. 2D). Therefore, combined with results shown in Fig. 1, Cav-$1^{-/-}$ mice may have been more resistant to HSV-1 infection because of enhanced elimination of virus and milder damage in the lungs.

Cav-1 facilitates virus replication in the lungs. Since Cav-1 may act as a gateway for the entry of viruses, such as SV40, we tested whether the milder lung pathology in Cav-1-deficient mice was a result of a lower entry of HSV-1. We analyzed viral load in DNA derived from lung cells at 4 h postinfection. As illustrated in Fig. 3A, no significant difference in the viral load inside the lung cells of Cav-$1^{-/-}$ and WT mice was observed after i.n. infection ($P = 0.67$).

On the other hand, a notable role of Cav-1 is its involvement in virus replication (29). We therefore tested if Cav-1 influenced HSV-1 replication in the lungs. To address this, mice were challenged with a lower dose of HSV-1 (1 LD_{50}). After 1, 3, and 5 days of infection, the genomic DNA of lung cells and whole lung protein was collected, and we examined viral load by qPCR and HSV-1 protein levels by Western blot. Increases in both viral load and glycoprotein D expression in the lung cells of WT mice were observed at 1 and 3 dpi compared to those in Cav-$1^{-/-}$ mice (Fig. 3B and C). The increased viral load in Cav-1 KO mice was not statistically significant from that of WT mice at day 3 p.i. Viruses were also cleared in both groups by 5 dpi, probably because C57BL/6 mice are resistant to low doses of viral infection. In addition, the viruses isolated from the challenged mice were quantified by measuring the $TCID_{50}$ in Vero cells. Figure 3D shows that Cav-1 expression drastically increased the viral load in the lungs (5.33 ± 0.44 $\log_{10}$ $TCID_{50}$ in WT versus 3.27 ± 0.501 $\log_{10}$ $TCID_{50}$ in Cav-$1^{-/-}$) but not in the brain at 7 dpi. Histochemical analysis of the expression of HSV-1 proteins showed a similar trend (Fig. 3E and F), further suggesting that Cav-1 facilitates virus replication. These results indicate that the greater resistance of Cav-$1^{-/-}$ lungs to HSV-1 infection was associated with inhibition of virus replication.

The effect of Cav-1 deficiency is dendritic cell dependent. The lung is one of the organs most affected by acute HSV-1 infection. DCs, macrophages, and epithelial cells of the lung have been reported to play critical roles in viral infection (38, 39). Therefore, we next examined these cellular populations, which might have been responsible for the increased resistance of Cav-$1^{-/-}$ mice. Both WT and Cav-$1^{-/-}$ mice were challenged with 10 LD_{50} of HSV-1. The viral loads in isolated DCs, macrophages, and epithelial cells were determined at 3 dpi. No difference in viral load was observed in macrophages and epithelial cells between the Cav-$1^{-/-}$ and WT groups. However, DCs from Cav-$1^{-/-}$ mice showed a significantly lower viral load than that of the WT DCs (Fig. 4A). To further assess this, $CD11c^+$ DCs were isolated from WT and Cav-$1^{-/-}$ mice and infected at an MOI of 5 for 24 h and 48 h *in vitro*. Viral load was substantially reduced in Cav-$1^{-/-}$ DCs compared to that in WT DCs (Fig. 4B), suggesting that DCs played a role against HSV-1 infection, but the role was limited by the Cav-1 protein. In addition, there was little difference between WT and Cav-$1^{-/-}$ mice in the number of DCs recruited to the lungs (data not shown), indicating Cav-1 does not influence DC migration to the lungs. To further elucidate the function of Cav-1 expressed by lung DCs during HSV-1 infection, a Cav-1 knockdown DC2.4 cell line (Cav-1^{kd} DCs) and a Cav-1 overexpression DC cell line (Cav-

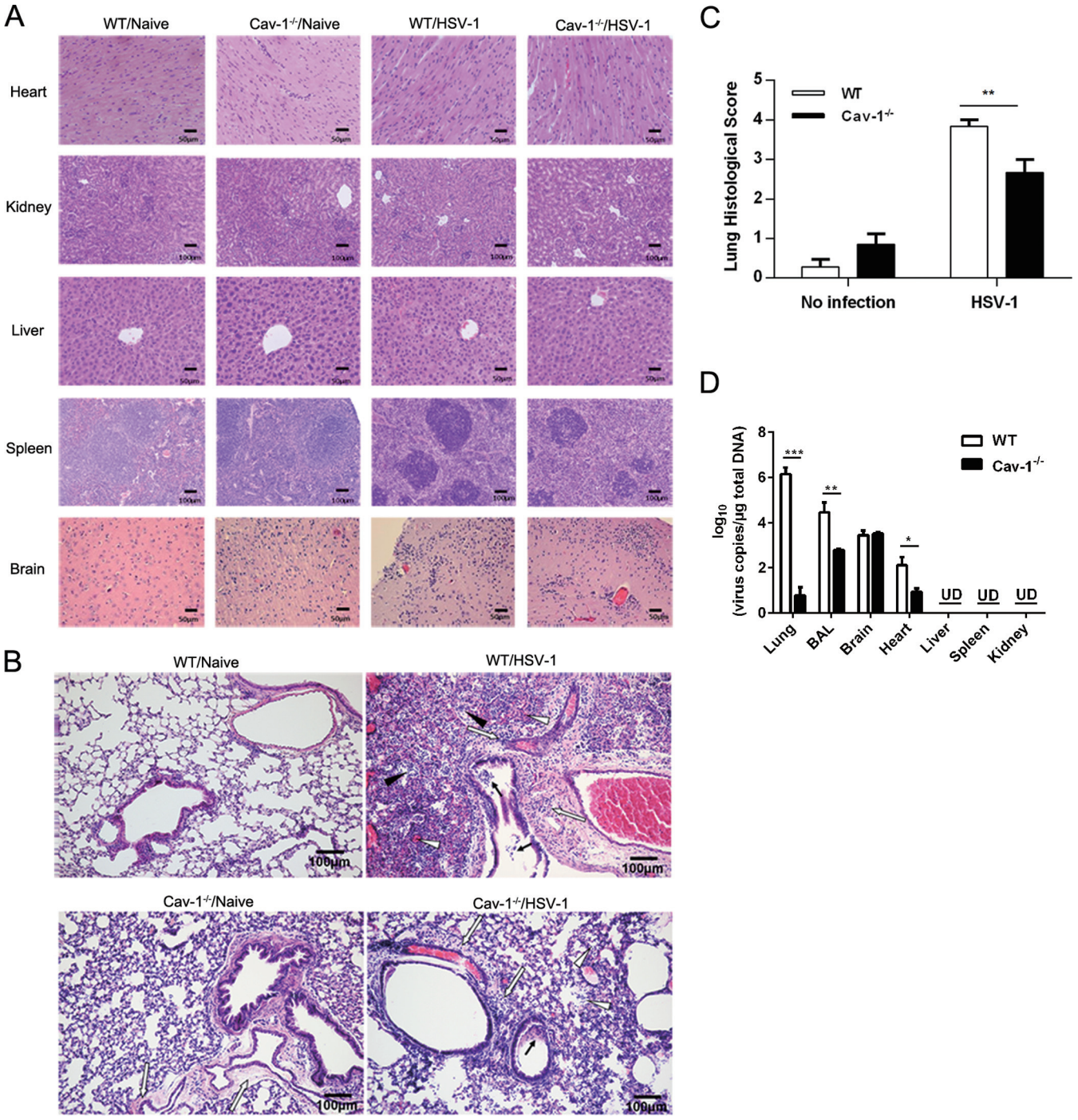

FIG 2 Cav-1 deficiency results in reduced viral replication and lung pathology. WT and Cav-1$^{-/-}$ mice were challenged with 10 LD_{50} of HSV-1. Next, the heart, liver, spleen, kidneys, lungs, and brain were separated at 7 dpi. $n = 6$. (A) Representative H&E-stained thin sections of organs (other than lung) from infected and uninfected mice. The bars indicate 50 μm or 100 μm. (B) Representative histopathology in the left lobe of the lung from infected and uninfected mice. Indicated are inflammatory cells infiltrating bronchial lumen (black arrows), edema and inflammatory cell infiltrations around the bronchi and vessels (white arrows), alveolar septum capillary congestion (open triangles), and inflammatory cells infiltrating alveolar space (black triangles). H&E stain was used. Scale bar indicates 100 μM. (C) Histological scores of the lung pathology in panel B. Severity of lung damage was assessed by the eye, scored, and analyzed. (D) Viral load in the infected organs. Total genomic DNA was extracted and the viral load assessed by qPCR. All data are representative of three independent experiments. UD, undetermined; *, $P < 0.05$; **, $P < 0.01$; ***, $P < 0.001$.

1^{over} DCs) were constructed. The differential expression of Cav-1 in these cell lines was confirmed by Western blot (Fig. 4C). The genetically modified DCs were infected with HSV-1 at an MOI of 5 for 2 h *in vitro* and then treated with mitomycin C at 50 μg/ml for 20 min at 37°C to prevent uncontrolled proliferation. A total of 2×10^6 cells in 50 μl of DMEM were adoptively transferred into the lungs of WT or Cav-1$^{-/-}$ recipients by i.t. injection. Twelve hours later, mice were i.n. infected with 10 LD_{50} of HSV-1, and

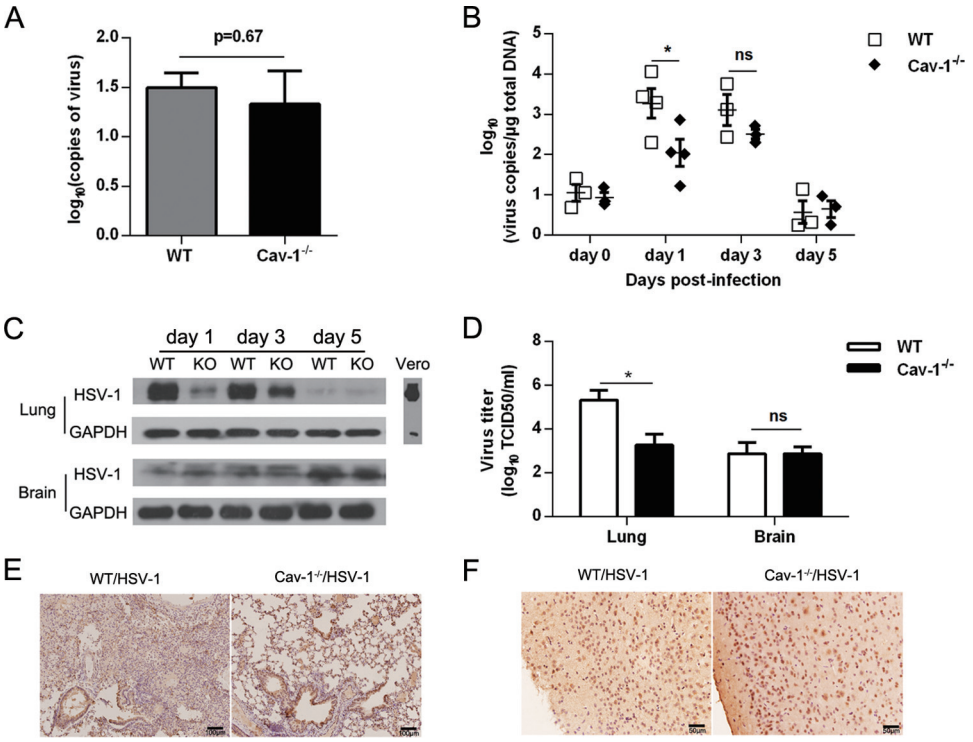

FIG 3 Cav-1 facilitates virus replication in lung cells. (A) Viral load in WT and Cav-1$^{-/-}$ lung cells 4 h after infection with 1 LD_{50} *in vitro*. The Pol gene content in total extracted DNA was determined by qPCR analysis. (B and C) Viral load in infected mice. Cells were separated from WT and Cav-1$^{-/-}$ mice at 0, 1, 3, and 5 days after infection with 1 LD_{50} of HSV-1. (B) Viral load in lung cells assessed by qPCR. (C) Amount of HSV-1 glycoprotein D in pooled whole-cell lysates of isolated lung and brain cells. Immunoblots of lysates were stained with Abs specific for glycoprotein D or GAPDH as a reference. Total proteins of HSV-1-infected Vero cells were loaded as a control. KO refers to Cav-1$^{-/-}$ mice. (D to F) Results from mice that were challenged with 10 LD_{50} of HSV-1 and examined at 7 dpi. (D) Viral load in lungs and brain quantified as $TCID_{50}$ in Vero cells according to the readout at day 4. (E and F) Representative immunohistochemical staining of HSV-1 in lung (E) and brain (F) sections. The scale bars on the sections indicate 100 μM for lungs and 50 μM for brain. The data are representative of three independent experiments. Student's *t* test was applied for differences between two groups. Two-way ANOVA was also applied. Nonsignificant (ns), $P > 0.05$; *, $P < 0.05$; **, $P < 0.01$; ***, $P < 0.001$.

survival was monitored as outlined in Fig. 4D. The WT mice that received Cav-1^{kd} DCs had a significantly increased survival of 33% at 8 dpi, whereas WT mice that received Cav-1^{over} DCs were all dead at 4 dpi (Fig. 4E). As HSV-1 infection might lead to body weight loss and Cav-1$^{-/-}$ mice are resistant to a lethal dose of HSV-1 infection, weight loss in Cav-1$^{-/-}$ mice was monitored and the function of Cav-1^{kd} DCs evaluated during HSV-1 infection. Infected Cav-1$^{-/-}$ mice that received Cav-1^{kd} DCs also showed growth and body weight gains similar to those of noninfected Cav-1$^{-/-}$ mice (Fig. 4F). In contrast, transfer of the Cav-1^{over} DCs into infected Cav-1$^{-/-}$ mice was accompanied by substantial weight loss (about 2.8 g decrease by day 11; Fig. 4F).

To further investigate the critical role of endogenous DCs during HSV-1 infection, mice lacking both Cav-1 and DCs (CD11c-DTR/Cav-1$^{-/-}$ [double knockout {DKO} mice]) were generated; the WT, CD11c-DTR, Cav-1$^{-/-}$, and DKO mice were challenged with 10 LD_{50} of HSV-1, and then the CD11c^{+} DC population was transiently depleted by DT injection. The survival of these mice was monitored over 12 days. Although the depletion efficiency of CD11c^{+} DCs is different in various organs, DT depletion shows a systemic depletion effect (40). The efficiency of depletion of CD11c^{+} DCs was assessed by flow cytometry at 24 h after injection. The CD11c^{+} DC population was successfully reduced to 0.014% by DT treatment (Fig. 4G). As shown in Fig. 4H, the survival rate was significantly impaired in DC-depleted DKO mice (0% at 6 dpi) relative to Cav-1 single-deficient mice (75% at 6 dpi), and mortality rates returned to a level comparable to that of infected CD11c-DTR mice. Our data demonstrate that DCs are capable of, and essential for, immune defense against HSV-1 infection, but their antiviral function is downregulated by HSV-1 via Cav-1.

Cav-1 suppresses NO production by DCs during HSV-1 infection. Since DCs lacking Cav-1 might confer resistance to HSV-1 infection, we next explored which cytokines or other mediators were involved. The levels of IL-6 and tumor necrosis factor alpha (TNF-α) in BALF were tested at days 0 and 4 postinfection. However, HSV-1 stimulated similar production of IL-6 and TNF-α in both WT and Cav-1$^{-/-}$ mice at 4 dpi (Fig. 5A). When the mRNA levels of antiviral cytokines and signaling molecules (IFN-β, IL-1β, IL-10, CD40, COX-2, PD-L1, ERK1, eNOS, and SOCS-1) in HSV-1-infected lung cells were measured at 1 and 3 dpi, no significant changes were observed, except for iNOS (Fig. 5B and C). iNOS, as an antiviral factor, is potently induced in virus-infected cells. We found that the mRNA level of iNOS was significantly augmented in Cav-1$^{-/-}$ lung cells but slowed in WT lung cells at 1 dpi ($P = 0.0015$) and 3 dpi ($P = 0.0168$), as depicted in Fig. 5C. Consistent with this, the iNOS mRNA level was also more strongly increased *in vitro* in freshly purified Cav-1$^{-/-}$ DCs than in WT DCs at 12, 24, and 36 hpi (Fig. 5D). Furthermore, as shown in Fig. 5E, Cav-1^{kd} DCs had a much greater abundance of

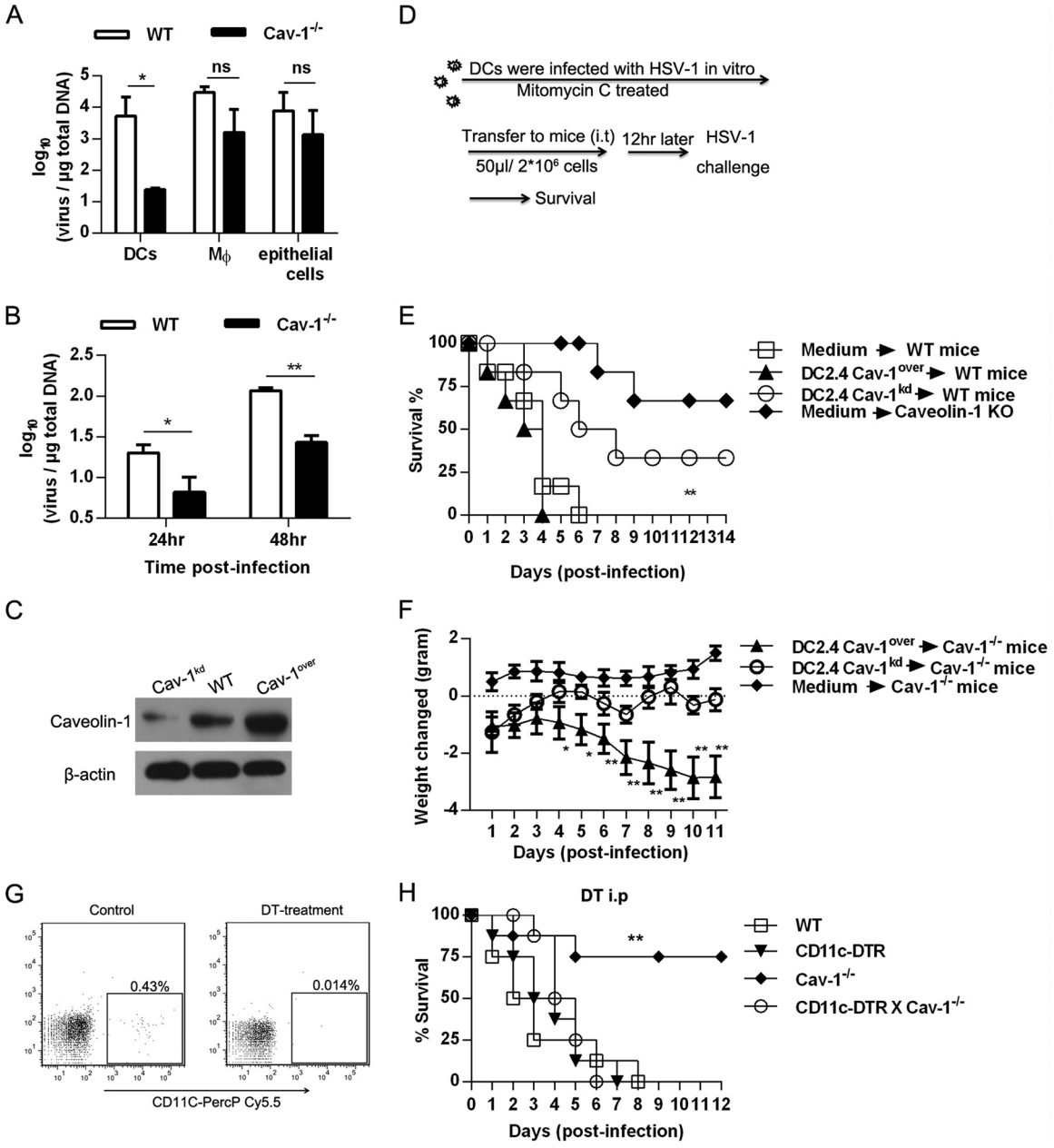

FIG 4 Cav-1$^{-/-}$-enhanced survival is DC dependent. (A) Viral load in DCs, macrophages (Mϕ), and epithelial cells from HSV-1-infected WT and Cav-1$^{-/-}$ mice. Mice were challenged with 10 LD_{50} HSV-1, cells were collected from the lungs at 3 dpi, genomic DNA was extracted, and the viral load was assessed by qPCR. (B) Viral load in DCs that were infected *in vitro*. DCs were isolated from WT and Cav-1$^{-/-}$ mice with the CD11c MicroBeads kit, infected with HSV-1 at an MOI of 5, and the total DNA was extracted at 24 hpi and 48 hpi for qPCR. (C) Cav-1 protein expression levels in recombinant DC2.4 cell lines. Cav-1 knockdown (Cav-1^{kd}) and Cav-1 overexpression (Cav-1^{over}) DC2.4 cell lines were constructed. Thirty micrograms of whole-cell extract was subjected to electrophoresis on an SDS-PAGE gel, transferred to a PVDF membrane, and the Cav-1 protein was assessed by Western blotting, with β-actin as control. (D) Outline protocol of i.t. adoptive transfer of Cav-1^{kd} DCs and Cav-1^{over} DCs. (E and F) Effect of caveolin-1 on resistance of mice to challenge with 10 LD_{50} of HSV-1. (E) Survival curves. Survival was enhanced in caveolin-1 KO mice and in mice receiving i.t. DC2.4 in which caveolin-1 expression was reduced (Cav-1^{kd}). Survival was decreased in mice receiving DC2.4 overexpressing caveolin-1 (Cav-1^{over}). The reference mice received i.t. DMEM. $n = 6$ mice per group. (F) Body weight change curves. Weight was determined daily after a lethal dose of HSV-1 in Cav-1$^{-/-}$ mice that received recombinant DC2.4 lines i.t. The reference Cav-1$^{-/-}$ mice received medium only and were not infected. (G) Efficiency of DC depletion by DT in CD11c-DTR mice. DT was injected i.p. in 8-ng/g doses at 12-h intervals. Peripheral blood mononuclear cells (PBMC) were collected at 24 hpi and stained with CD11c-PercP-Cy5.5. Next, flow cytometry was performed to detect the percentage of DCs. (H) Resistance of Cav-1$^{-/-}$ mice after DC depletion. WT, CD11c-DTR, Cav-1$^{-/-}$, and DKO mice were pretreated with DT and i.n. challenged with 10 LD_{50} of HSV-1. $n = 6$. DT injections were performed at 12-h intervals during infection. **, Cav-1$^{-/-}$ versus DKO. The results are presented as the mean ± SEM from three independent experiments. For survival curve analysis, a log rank (Mantel-Cox) test was performed. Nonsignificant (ns), $P > 0.05$; *, $P < 0.05$; **, $P < 0.01$.

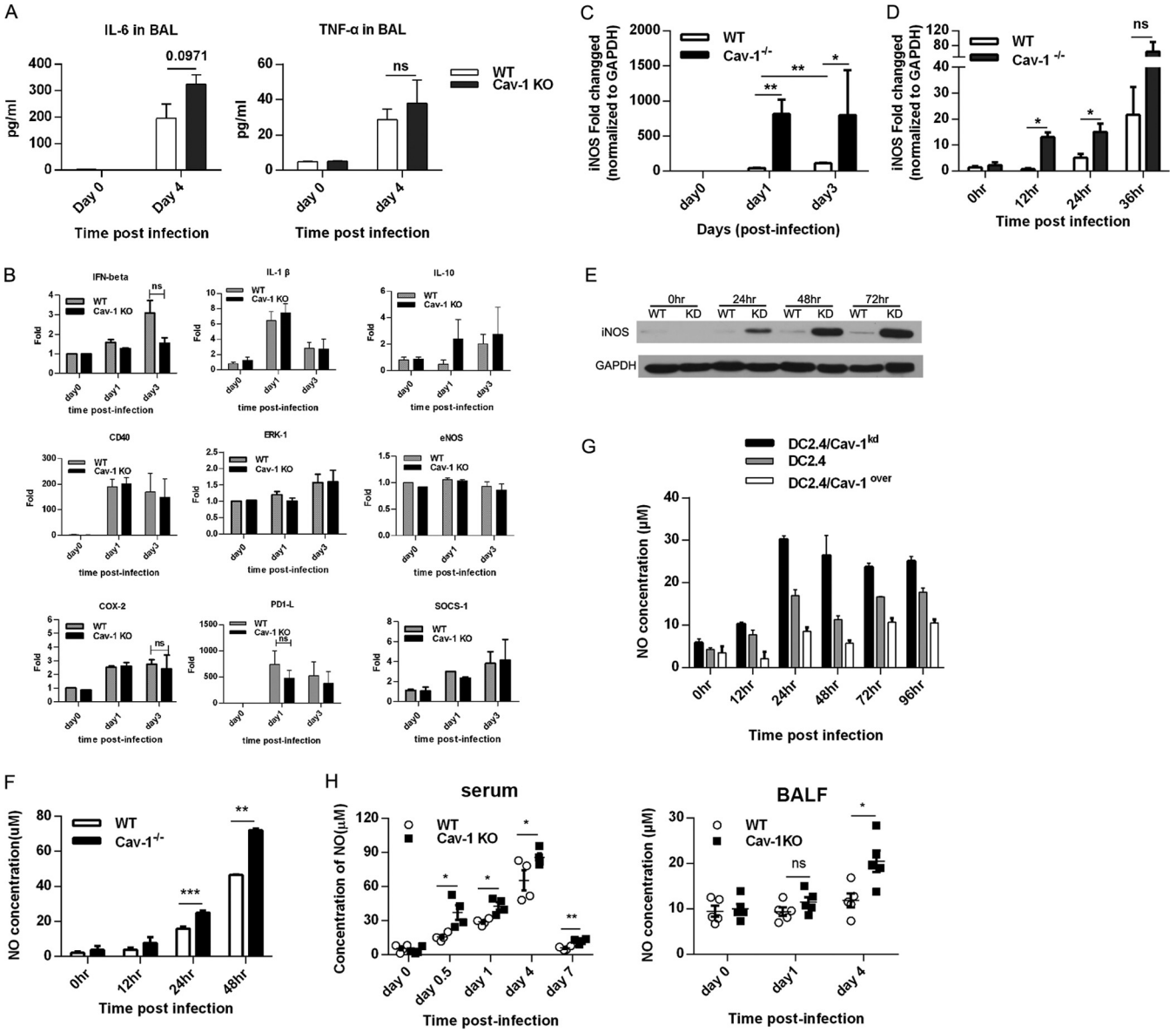

FIG 5 Cav-1 suppresses NO production by DCs during HSV-1 infection. (A to C) Cytokine and NO production in lungs of infected WT and Cav-1$^{-/-}$ mice. Mice were infected with 10 LD_{50} HSV-1, and BALF was collected 0 to 4 dpi. (A) IL-6 and TNF-α in BALF quantified with the cytometric bead assay with specific antibody-conjugated beads. (B and C) Inflammatory cytokine, chemokine, and iNOS expression in BAL lung cells. Cells were collected at 0, 1, and 3 dpi, total RNA was extracted, and mRNA expression was assessed by qPCR. The fold induction relative to GAPDH is shown. (B) Expression of cytokines and chemokines. (C) Expression of iNOS. (D) Expression of iNOS in CD11c^{+} DCs purified from WT and Cav-1$^{-/-}$ mice and then infected with HSV-1 at an MOI of 5. The fold changes of iNOS expressions were normalized to GAPDH. (E) iNOS protein increase in HSV-1-infected Cav-1^{kd} DCs and not in WT DCs. Total cell protein was extracted for Western blot analysis at 0, 24, 48, and 72 hpi. iNOS and GAPDH expression levels were detected with specific antibodies. (F) NO levels in supernatants of CD11c^{+} DCs that had been purified from WT and Cav-1$^{-/-}$ mice and infected with HSV-1 at an MOI of 5. (G) NO levels in supernatants of WT (DC2.4), Cav-1^{kd}, and Cav-1^{over} DCs after infection with HSV-1 at an MOI of 5. (H) NO levels in serum and BALF of 10 LD_{50} infected WT and Cav-1$^{-/-}$ mice. In each panel, the data shown are representative of three independent experiments. Nonsignificant (ns), $P > 0.05$; *, $P < 0.05$; **, $P < 0.01$; ***, $P < 0.001$.

iNOS protein than did WT DCs at 24, 48, and 72 hpi *in vitro*, and at 48 hpi, the release of NO from Cav-1$^{-/-}$ DCs was 1.56-fold greater than that from the WT cells (Fig. 5F). The dynamics of NO release were associated with the change in expression of Cav-1. The DCs with silenced Cav-1 exhibited a peak production of NO at ~30 μM at 24 hpi, whereas the WT counterpart peak was at 16.7 μM, and the peak for Cav-1-overexpressed DCs was at 8.6 μM (Fig. 5G), indicating that the degree of NO release was strongly associated with the level of Cav-1 expression. To further confirm the retardation of the expression of NO by Cav-1, the NO levels in serum and BALF were analyzed. In agreement with the results *in vitro*, there was significantly less NO at 0.5, 1, and 4 dpi in the serum and in BALF of WT mice than that in the Cav-1$^{-/-}$ counterparts (Fig. 5H). Furthermore, as Cav-1 regulated the production of NO during HSV-1 infection, the penetration of virus entry in Cav-1-deficient DCs needs to be evaluated. The results showed the virus entry into DCs was not significantly changed in Cav-1 knockdown DCs at an MOI of 0.5, 1, and 5 (data not shown),

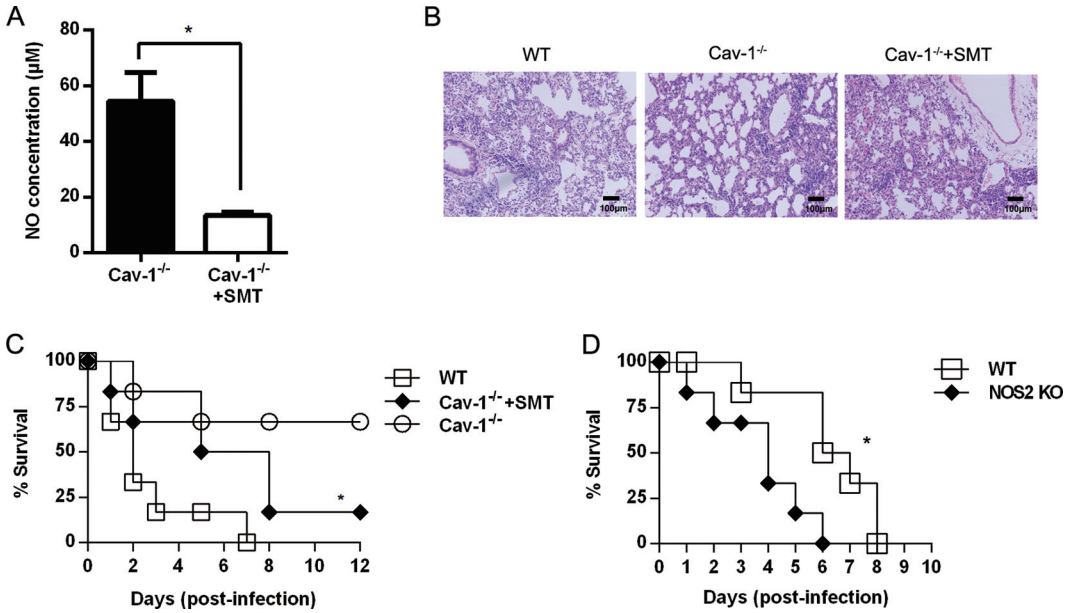

FIG 6 Decreased NO and increased mortality in SMT-treated Cav-$1^{-/-}$ mice. Mice were challenged by 10 LD_{50} of HSV-1 i.n. and given daily i.p. injections of the iNOS inhibitor (50 mg/kg), as described in Materials and Methods. (A) Serum levels of NO in the SMT-treated and nontreated Cav-$1^{-/-}$ mice. (B) Histopathology in lung sections stained with H&E stain. The scale bar is 100 μm. (C) Percentage of survival. *, $P < 0.05$ between SMT-treated and nontreated Cav-$1^{-/-}$ groups. $n = 6$. (D) Survival of iNOS KO mice and WT mice after i.n. challenge with 10 LD_{50} of HSV-1. The mice were observed daily. The data are representative of two independent experiments. *, $P < 0.05$.

which indicated that Cav-1-mediated HSV-1 entry into DCs resulted in the impairment of NOS2 activity by mechanisms that were Cav-1 dependent. Collectively, these findings indicate that Cav-1 suppresses NO production by DCs during HSV-1 infection, which may be responsible for the greater susceptibility of WT mice to HSV-1 infection.

Inhibition of iNOS with SMT abolishes the resistance of Cav-$1^{-/-}$ mice to HSV-1 challenge. Since NO was reported to inhibit HSV-1 infection (17), lower production of NO might account for greater viral reproduction and exacerbated mortality in WT compared to that in Cav-$1^{-/-}$ mice. We found that daily i.p. administration of SMT (iNOS inhibitor) to Cav-$1^{-/-}$ mice during the course of HSV-1 infection resulted in a significantly smaller amount of NO in serum at 48 hpi (Fig. 6A). In keeping with previous data, the lungs of SMT-treated Cav-$1^{-/-}$ mice exhibited pathological changes of greater severity than that in the nontreated Cav-$1^{-/-}$ mice (Fig. 6B). Consistent with the histological data, this inhibition of iNOS with SMT nearly abolished the Cav-$1^{-/-}$-mediated protection against HSV-1 infection ($P = 0.03$) (Fig. 6C). Furthermore, mice lacking iNOS (NOS2 KO) were significantly more susceptible to lethal HSV-1 infection than WT ($iNOS^{+/+}$) mice ($P = 0.019$) (Fig. 6D). We conclude that NO is involved in the resistance of Cav-$1^{-/-}$ mice and alleviates the lung pathology generated by HSV-1 infection.

Colocalization of HSV-1 with Cav-1 and iNOS in caveolae. Since Cav-1 modulated iNOS activity in HSV-1-infected DCs, we investigated the subcellular localization of these proteins. Confocal microscopy showed that 2 h after infection of DCs, HSV-1 colocalized with Cav-1 in caveolae, the cytoplasm, and membranes (Fig. 7A). In addition, HSV-1-induced iNOS was observed to colocalize with Cav-1 in caveolae at 24 hpi (Fig. 7B). Furthermore, immunoprecipitation indicated that there might be protein-protein interactions between Cav-1 and iNOS in the caveolae and that this interaction increases as infection progresses (Fig. 7C).

DISCUSSION

Since Cav-1 modulates HSV-1 replication in infected cells, it appears to be an important component of cell defense. However, the molecular cross talk that mediates the effect of Cav-1 on antiviral activity is largely unknown. In this study, we uncovered a novel mechanism exploited by HSV-1, using Cav-1 to disarm the production by DCs of the antiviral factor NO. We showed that deficiency of Cav-1 protected mice from fatal HSV-1 infection, resulting in much milder lung morphological changes and a lower level of viral load. The resistance of Cav-$1^{-/-}$ mice against virus infection was DC dependent. Mechanistic studies demonstrated that the functions of Cav-1 include negatively regulating the production of iNOS and NO in DCs. Depletion of $CD11c^{+}$ DCs in Cav-$1^{-/-}$ mice or iNOS inhibition by SMT significantly impaired the production of NO and diminished the resistance conferred by the Cav-$1^{-/-}$ state. Furthermore, we observed that Cav-1 expression colocalized with iNOS and sequestered together with virus in caveolae in HSV-1-infected DCs. Therefore, this study identified a previously unrecognized role of Cav-1 during HSV-1 infection in the lungs. We demonstrated for the first time that Cav-1 facilitates HSV-1 infection and leads to lung injury and mortality by retardation of the NO response in the lung DCs.

Although caveolae are best known as an important regulatory element for lipid metabolism, recent studies suggested that caveolae, and particularly the Cav-1 structural protein, can be involved in the internalization of pathogens, signal transduction, and host defenses (19, 26). Indeed, previous studies have demonstrated that Cav-1 facilitates H1N1 and HBV virus replication in cell cul-

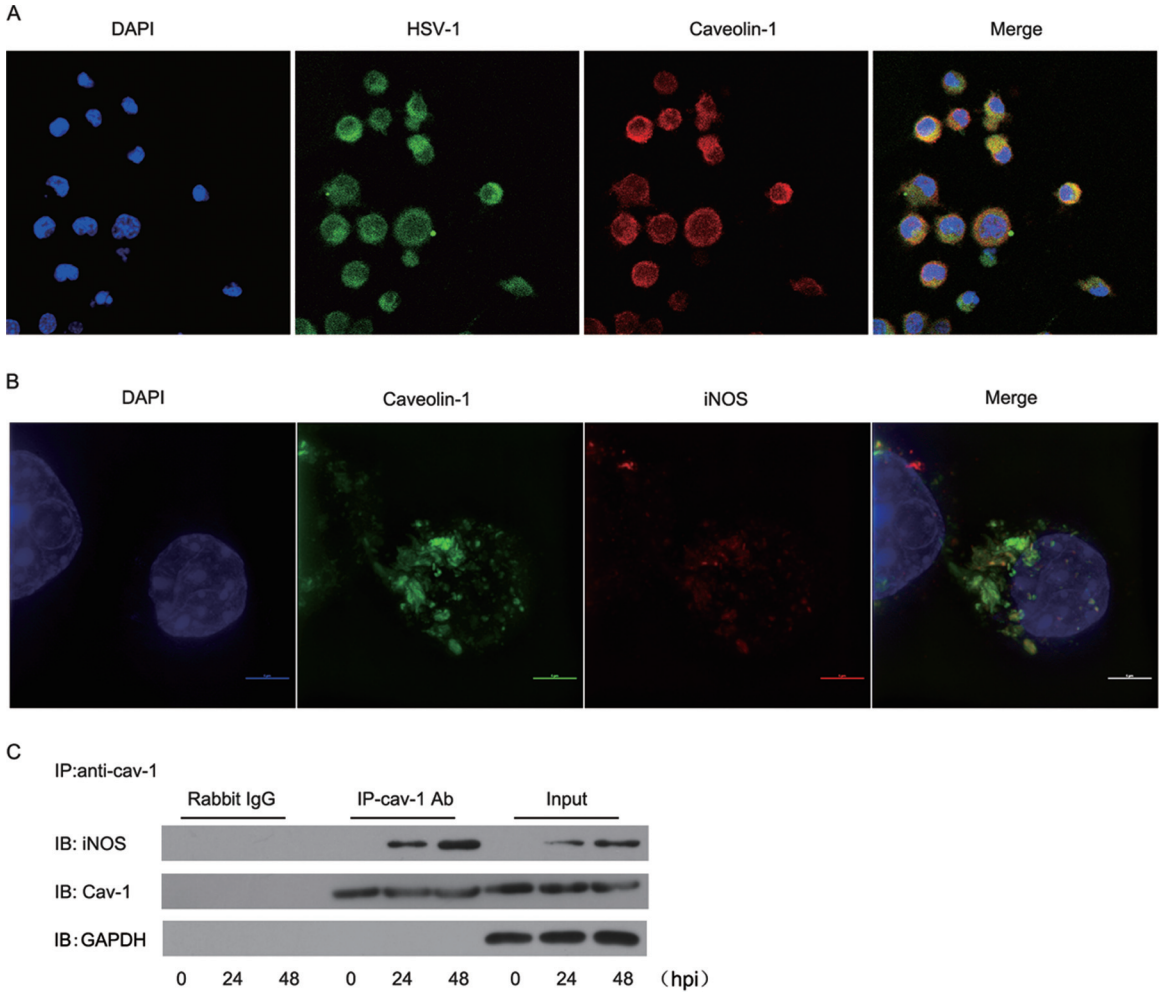

FIG 7 Cav-1 sequesters iNOS in caveolae in HSV-1-infected DCs. (A) Localization of HSV-1 in caveolae. DC2.4 cells were infected at an MOI of 50 and stained at 2 hpi with goat anti-HSV-1 and rabbit anti-Cav-1 antibodies. Confocal microscopy was performed after secondary goat-anti-rabbit IgG-PE and bovine anti-goat-FITC antibody staining. (B) Localization of iNOS in caveolae. DC2.4 cells were infected at an MOI of 5 and stained 24 hpi with goat anti-iNOS antibody, followed by bovine anti-goat-PE. Bar, 5 μm. (C) Coimmunoprecipitation (Co-IP) of Cav-1 with iNOS. DCs were infected with HSV-1 at an MOI of 5 and lysed at different times with IP/wash lysis buffer. The lysate contents of iNOS, Cav-1, and GAPDH proteins were determined by Western blot analysis with specific Abs. Input, lysate before immunoprecipitation; IB, immunoblot; IP-Cav-1 Ab, immunoprecipitate; rabbit IgG, negative control. Similar results were obtained in two additional independent experiments.

ture (29, 30), and Cav-1 was found to regulate cytokine expression in macrophages via the p38/mitogen-activated protein kinase (MAPK) pathway (41). However, the role of Cav-1 in herpesvirus infection is largely unclear. To investigate this, we first established an i.n. HSV-1 challenge system in C57BL/6 WT and Cav-1$^{-/-}$ mice and found that the induction of significant mortality caused by i.n. infection required a dose of 9.47 $\log_{10}$ $TCID_{50}$ of HSV-1 in WT mice (Fig. 1A), although only 8.47 $\log_{10}$ $TCID_{50}$ was required by intraperitoneal (i.p.) challenge (data not shown). WT animals that were heavily challenged i.n. with 10 LD_{50} of HSV-1 all died, while Cav-1$^{-/-}$ mice exhibited 75% protection (Fig. 1B), revealing that Cav-1 played a suppressive role in host immunity during HSV-1 infection via the i.n. route.

HSV-1 spreads to the brain, lungs, liver, spleen, and other tissues after i.n. infection, causing encephalitis, pneumonia, hepatitis, and keratitis (42). Although it mainly infects the nervous system and induces encephalitis in mice, HSV-1-induced pneumonia is common in immunocompromised patients, newborns, healthy persons, and mice (5, 7). Accordingly, when we used a high titer of HSV-1 (10 LD_{50}) to infect mice via the i.n. route, this resulted in severe disease in the lungs, with edema formation and alveolar septum capillary congestion. In contrast, in Cav-1$^{-/-}$ mice, there was remarkably less pneumonitis induced by the HSV-1 infection, consistent with their increased survival (Fig. 2B and C). Previous studies noted that both imbalanced host immune responses and viral pathogenic factors are critical for virus-induced pneumonia (4, 43). In agreement with evidence that Cav-1 might facilitate virus replication (29), we observed that the expression of Cav-1 significantly elevated HSV-1 titers in lung cells and BALF. Interestingly, although the i.n. infection by HSV-1 also induced encephalitis in the brain, there were no significant differences between the Cav-1$^{-/-}$ and WT mice in either degree of pathology (Fig. 2A) or viral load (Fig. 3D to F). The different effect of Cav-1 on organs (brain versus lungs) might due to the extremely high dose of HSV-1 and the route of infection (intranasal injection). The different expression of Cav-1 in epithelial cells of

lung and brain cells may also contribute to the differences, and this needs to be investigated further. We concluded that the lungs were selectively susceptible after i.n. infection and that the pathology and viral load were enhanced by Cav-1 availability. The HSV-1 infection-induced pneumonitis in WT C57BL/6 mice was therefore adopted as a model system to further define the role of Cav-1.

Although the mechanisms and types of cells mediating resistance against HSV-1 infection in lungs are ill defined, published studies suggest that certain cell subsets of the innate immune system may be involved in controlling virus replication (44, 45). DCs, macrophages, and epithelial cells form the first line of host defense in lungs against invading pathogens, like HSV-1, lymphocytic choriomeningitis virus (LCMV), and influenza A (43, 46–48). In the case of RSV-induced pneumonia, adoptive transfer of DCs contributed to a reduction of RSV and Sindbis virus titers, with limited virus replication and airway hyperresponsiveness (49, 50). Previous studies of HSV-1 infection showed that an ablation of $CD11c^+$ DCs *in vivo* increased susceptibility to infection (47), but the role that DCs play during HSV-1 infection required clarification. Our results shown in Fig. 4A and B clearly show that the absence of Cav-1 significantly suppressed infection in lung DCs but not in lung macrophages or epithelial cells. Studies showed $iCD8^+$ DCs isolated from *Mycobacterium bovis* BCG-infected mice were adoptively transferred to mice and both enhanced bacterial clearance and reduced pathological reactions following challenge. But the noninfected CD8 DC control and PBS sham treatment exhibited no improvement in bacterial load in the lungs (51). In addition, DC pretreatment is able to initiate T-cell immune responses against malaria and viruses in mice (52, 53). In the experiment outlined in the Fig. 4, DCs were preinfected with HSV-1 before adoptive transfer. The importance of the DCs was further supported by our adoptive transfer experiments:, as WT mice that received the Cav-1^{kd} DCs showed better survival at 8 dpi (33%) than that of mice that received Cav-1^{over} DC (0% survival at 4 dpi; Fig. 4E). Mitomycin C was applied to avoid unlimited DC2.4 cell proliferation before the transfer (54). Previous studies showed that mitomycin C treatment blocked cellular DNA integration but did not affect Visna virus and SV40 replication (55, 56). In addition, the extent of T-cell stimulation by mitomycin C-treated DCs is dose dependent, indicating that the function of mitomycin C is diverse and needs to be studied in the future (57). The depletion of DCs in Cav-$1^{-/-}$ mice also abolished the protective effect that was conferred by the absence of Cav-1 (Fig. 4H). Our findings indicated that HSV-1 exploits Cav-1 to disarm the antiviral effects of DCs in lungs.

Cells in the innate immune system are equipped with antiviral molecules for the clearance of invading pathogens. Proinflammatory and inflammatory cytokines are key regulators of the innate cellular defense against viral infections and might be the determining factors against respiratory infections, including HSV-1, H1N1, and respiratory syncytial virus (RSV) (58–60). NO is a product of the cellular immune system that is well known as a reactive free radical molecule that modulates cytokine expression, and it is beneficial to the host defense against virus infections (61). For example, cells with iNOS inhibited by 1-NG-monomethyl arginine (1-NMMA) failed to restrict Japanese encephalitis virus (JEV) replication (62), and IFN-γ-induced iNOS and NO production inhibited the replication of vaccinia virus (VV) and HSV-1 (17, 63). Our observations implicating NO in resistance to HIV-1 are consistent with this. We observed that the deficiency of Cav-1 markedly enhanced iNOS and NO production in BALF and in DCs during HSV-1 infection (Fig. 5). In addition, lower levels of NO were observed in infected DC-depleted mice (data not shown) and in the serum from SMT-treated Cav-$1^{-/-}$ mice (Fig. 6A) than those in Cav-$1^{-/-}$ mice and are associated with higher mortality. Thus, consistent with a general antiviral role for iNOS, NO from lung DCs appears to be the key to resistance to HSV-1 infection. Furthermore, the connection between Cav-1 and iNOS has been documented in cells responding to LPS stimulation and in a tumorigenesis model (32, 34). Based on these observations, we hypothesized that HSV-1 disarms DCs by using Cav-1 to reduce iNOS production of NO.

Although IL-6 and TNF-α have been reported to play critical roles in immunity against HSV-1 (64), in this study, the deficiency in Cav-1 resulted in only slightly upregulated the expression of IL-6 and TNF-α in BALF, and this was not statistically significant (Fig. 5A). On the other hand, we did observe that Cav-1 upregulated transforming growth factor beta 1 (TGF-β1) expression in total lung cells (data not shown). Because TGF-β1 is a suppressive factor during immune responses, it may repress the expression of iNOS or other antiviral molecules and thereby contribute to virus replication (65). Whether Cav-1 regulation of TGF-β1, IL-6, or TNF-α is involved in resistance to HSV-1 infection in lungs needs further study.

We propose that HSV-1-induced NO production was suppressed through iNOS sequestration in caveolae. Our observations that Cav-1 both suppressed iNOS expression and colocalized with iNOS and HSV-1 in infected DC cells (Fig. 7B and C) is consistent with recent reports: in an LPS-induced sepsis model, Cav-1 downregulated LPS-induced iNOS and NO production, resulting in aggravated lung edema formation (34, 41); in a human colon carcinoma model, Cav-1 was found to cofractionate with iNOS and detain iNOS protein in caveolae, leading to iNOS proteolysis (32). Since there is also evidence that SV40 uses caveolae as a gateway to mediate viral entry and avoid host antiviral responses (27, 66), it appears that HSV-1 may use such a gateway to cause sequestration and the consequent inactivation of iNOS in the caveolae of lung DCs.

In sum, in this study, we demonstrate that Cav-1 plays a key role in susceptibility to HSV-1 infection, with higher viral load and aggravated lung pathology occurring in its presence; a lack of Cav-1 reversed this susceptibility and provided stronger protection against HSV-1 infection. Notably, NO and DCs were found to be critically important to the host defense against HSV-1 infection in Cav-$1^{-/-}$ mice. Thus, this study provides a new insight into a novel immunity evasion mechanism of HSV-1 and might indicate a valuable approach to controlling herpesvirus infection.

ACKNOWLEDGMENTS

This work was supported in part by the National Science Foundation of China (31430027 and 30930068), MOST national 863 project of China (2012AA02A407), and the National Science and Technology Major Program of Infectious Diseases (2013ZX10002001) to Bin Wang.

We thank Jane Q. L. Yu, Zhonghuai He, and Xianghua Shi for their assistance in this work.

REFERENCES

1. **Qiu X, Zhong M, Xiang Y, Qu C, Pei Y, Zhang Y, Yang C, Gasteiger J, Xu J, Liu Z, Wang Y.** 2013. Self-organizing maps for the classification of gallic acylate polyphenols as HSV-1 inhibitors. Med Chem **10**:388–401.

2. **Wang Q, Guo J, Jia W.** 1997. Intracerebral recombinant HSV-1 vector does not reactivate latent HSV-1. Gene Ther **4:**1300–1304. http://dx.doi.org/10.1038/sj.gt.3300535.
3. **Altavilla G, Calistri A, Cavaggioni A, Favero M, Mucignat-Caretta C, Palu G.** 2002. Brain resistance to HSV-1 encephalitis in a mouse model. J Neurovirol **8:**180–190. http://dx.doi.org/10.1080/13550280290049633.
4. **Witt MN, Braun GS, Ihrler S, Schmid H.** 2009. Occurrence of HSV-1-induced pneumonitis in patients under standard immunosuppressive therapy for rheumatic, vasculitic, and connective tissue disease. BMC Pulm Med **9:**22. http://dx.doi.org/10.1186/1471-2466-9-22.
5. **Luyt CE, Combes A, Deback C, Aubriot-Lorton MH, Nieszkowska A, Trouillet JL, Capron F, Agut H, Gibert C, Chastre J.** 2007. Herpes simplex virus lung infection in patients undergoing prolonged mechanical ventilation. Am J Respir Crit Care Med **175:**935–942. http://dx.doi.org/10.1164/rccm.200609-1322OC.
6. **Costa C, Sidoti F, Saldan A, Sinesi F, Balloco C, Simeone S, Lorusso M, Mantovani S, Merlino C, Solidoro P, Cavallo R.** 2012. Clinical impact of HSV-1 detection in the lower respiratory tract from hospitalized adult patients. Clin Microbiol Infect **18:**E305–E307. http://dx.doi.org/10.1111/j.1469-0691.2012.03882.x.
7. **Adler H, Beland JL, Del-Pan NC, Kobzik L, Brewer JP, Martin TR, Rimm IJ.** 1997. Suppression of herpes simplex virus type 1 (HSV-1)-induced pneumonia in mice by inhibition of inducible nitric oxide synthase (iNOS, NOS2) J Exp Med **185:**1533–1540.
8. **de Jong MA, de Witte L, Bolmstedt A, van Kooyk Y, Geijtenbeek TB.** 2008. Dendritic cells mediate herpes simplex virus infection and transmission through the C-type lectin DC-SIGN. J Gen Virol **89:**2398–2409. http://dx.doi.org/10.1099/vir.0.2008/003129-0.
9. **Cook WJ, Kramer MF, Walker RM, Burwell TJ, Holman HA, Coen DM, Knipe DM.** 2004. Persistent expression of chemokine and chemokine receptor RNAs at primary and latent sites of herpes simplex virus 1 infection. Virol J **1:**5. http://dx.doi.org/10.1186/1743-422X-1-5.
10. **Frank GM, Buela KA, Maker DM, Harvey SA, Hendricks RL.** 2012. Early responding dendritic cells direct the local NK response to control herpes simplex virus 1 infection within the cornea. J Immunol **188:**1350–1359. http://dx.doi.org/10.4049/jimmunol.1101968.
11. **Kassim SH, Rajasagi NK, Zhao X, Chervenak R, Jennings SR.** 2006. *In vivo* ablation of CD11c-positive dendritic cells increases susceptibility to herpes simplex virus type 1 infection and diminishes NK and T-cell responses. J Virol **80:**3985–3993. http://dx.doi.org/10.1128/JVI.80.8.3985-3993.2006.
12. **Kohno S, Murata T, Sugiura A, Ito C, Iranshahi M, Hikita K, Kaneda N.** 2011. Methyl galbanate, a novel inhibitor of nitric oxide production in mouse macrophage RAW264.7 cells. J Nat Med **65:**353–359. http://dx.doi.org/10.1007/s11418-010-0505-7.
13. **Lu L, Bonham CA, Chambers FG, Watkins SC, Hoffman RA, Simmons RL, Thomson AW.** 1996. Induction of nitric oxide synthase in mouse dendritic cells by IFN-gamma, endotoxin, and interaction with allogeneic T cells: nitric oxide production is associated with dendritic cell apoptosis. J Immunol **157:**3577–3586.
14. **Vallance P, Moncada S.** 1993. Role of endogenous nitric oxide in septic shock. New Horiz **1:**77–86.
15. **Croen KD.** 1993. Evidence for antiviral effect of nitric oxide. Inhibition of herpes simplex virus type 1 replication. J Clin Invest **91:**2446–2452.
16. **Imanishi N, Andoh T, Sakai S, Satoh M, Katada Y, Ueda K, Terasawa K, Ochiai H.** 2005. Induction of inducible nitric oxide (NO) synthase mRNA and NO production in macrophages infected with influenza A/PR/8 virus and stimulated with its ether-split product. Microbiol Immunol **49:**41–48. http://dx.doi.org/10.1111/j.1348-0421.2005.tb03638.x.
17. **Gamba G, Cavalieri H, Courreges MC, Massouh EJ, Benencia F.** 2004. Early inhibition of nitric oxide production increases HSV-1 intranasal infection. J Med Virol **73:**313–322. http://dx.doi.org/10.1002/jmv.20093.
18. **Tucker PC, Griffin DE, Choi S, Bui N, Wesselingh S.** 1996. Inhibition of nitric oxide synthesis increases mortality in Sindbis virus encephalitis. J Virol **70:**3972–3977.
19. **Stuart ES, Webley WC, Norkin LC.** 2003. Lipid rafts, caveolae, caveolin-1, and entry by chlamydiae into host cells. Exp Cell Res **287:**67–78. http://dx.doi.org/10.1016/S0014-4827(03)00059-4.
20. **Volonté D, Galbiati F, Pestell RG, Lisanti MP.** 2001. Cellular stress induces the tyrosine phosphorylation of caveolin-1 (Tyr(14)) via activation of p38 mitogen-activated protein kinase and c-Src kinase. Evidence for caveolae, the actin cytoskeleton, and focal adhesions as mechanical sensors of osmotic stress. J Biol Chem **276:**8094–8103.
21. **Catalán V, Gómez-Ambrosi J, Rodríguez A, Silva C, Rotellar F, Gil MJ, Cienfuegos JA, Salvador J, Frühbeck G.** 2008. Expression of caveolin-1 in human adipose tissue is upregulated in obesity and obesity-associated type 2 diabetes mellitus and related to inflammation. Clin Endocrinol (Oxf) **68:**213–219.
22. **Pavlides S, Tsirigos A, Vera I, Flomenberg N, Frank PG, Casimiro MC, Wang C, Fortina P, Addya S, Pestell RG, Martinez-Outschoorn UE, Sotgia F, Lisanti MP.** 2010. Loss of stromal caveolin-1 leads to oxidative stress, mimics hypoxia and drives inflammation in the tumor microenvironment, conferring the "reverse Warburg effect": a transcriptional informatics analysis with validation. Cell Cycle **9:**2201–2219. http://dx.doi.org/10.4161/cc.9.11.11848.
23. **Li J, Geng S, Xie X, Liu H, Zheng G, Sun X, Zhao G, Wan Y, Wu Y, Chen X, Zhong Y, Wang B.** 2012. Caveolin-1-mediated negative signaling plays a critical role in the induction of regulatory dendritic cells by DNA and protein coimmunization. J Immunol **189:**2852–2859. http://dx.doi.org/10.4049/jimmunol.1102828.
24. **Huang WR, Wang YC, Chi PI, Wang L, Wang CY, Lin CH, Liu HJ.** 2011. Cell entry of avian reovirus follows a caveolin-1-mediated and dynamin-2-dependent endocytic pathway that requires activation of p38 mitogen-activated protein kinase (MAPK) and Src signaling pathways as well as microtubules and small GTPase Rab5 protein. J Biol Chem **286:**30780–30794. http://dx.doi.org/10.1074/jbc.M111.257154.
25. **Van Gorp H, Van Breedam W, Delputte PL, Nauwynck HJ.** 2009. The porcine reproductive and respiratory syndrome virus requires trafficking through CD163-positive early endosomes, but not late endosomes, for productive infection. Arch Virol **154:**1939–1943. http://dx.doi.org/10.1007/s00705-009-0527-1.
26. **Norkin LC, Kuksin D.** 2005. The caveolae-mediated sv40 entry pathway bypasses the golgi complex en route to the endoplasmic reticulum. Virol J **2:**38. http://dx.doi.org/10.1186/1743-422X-2-38.
27. **Pelkmans L, Kartenbeck J, Helenius A.** 2001. Caveolar endocytosis of simian virus 40 reveals a new two-step vesicular-transport pathway to the ER. Nat Cell Biol **3:**473–483. http://dx.doi.org/10.1038/35074539.
28. **Beer C, Andersen DS, Rojek A, Pedersen L.** 2005. Caveola-dependent endocytic entry of amphotropic murine leukemia virus. J Virol **79:**10776–10787. http://dx.doi.org/10.1128/JVI.79.16.10776-10787.2005.
29. **Sun L, Hemgård GV, Susanto SA, Wirth M.** 2010. Caveolin-1 influences human influenza A virus (H1N1) multiplication in cell culture. Virol J **7:**108. http://dx.doi.org/10.1186/1743-422X-7-108.
30. **Macovei A, Radulescu C, Lazar C, Petrescu S, Durantel D, Dwek RA, Zitzmann N, Nichita NB.** 2010. Hepatitis B virus requires intact caveolin-1 function for productive infection in HepaRG cells. J Virol **84:**243–253. http://dx.doi.org/10.1128/JVI.01207-09.
31. **Chidlow JH, Jr, Sessa WC.** 2010. Caveolae, caveolins, and cavins: complex control of cellular signalling and inflammation. Cardiovascular research **86:**219–225. http://dx.doi.org/10.1093/cvr/cvq075.
32. **Felley-Bosco E, Bender FC, Courjault-Gautier F, Bron C, Quest AF.** 2000. Caveolin-1 down-regulates inducible nitric oxide synthase via the proteasome pathway in human colon carcinoma cells. Proc Natl Acad Sci U S A **97:**14334–14339. http://dx.doi.org/10.1073/pnas.250406797.
33. **Felley-Bosco E, Bender F, Quest AF.** 2002. Caveolin-1-mediated post-transcriptional regulation of inducible nitric oxide synthase in human colon carcinoma cells. Biol Res **35:**169–176.
34. **Garrean S, Gao XP, Brovkovych V, Shimizu J, Zhao YY, Vogel SM, Malik AB.** 2006. Caveolin-1 regulates NF-kappaB activation and lung inflammatory response to sepsis induced by lipopolysaccharide. J Immunol **177:**4853–4860. http://dx.doi.org/10.4049/jimmunol.177.7.4853.
35. **Geng S, Zhong Y, Wang S, Liu H, Zou Q, Xie X, Li C, Yu Q, He Z, Wang B.** 2012. Amiloride enhances antigen specific CTL by faciliting [*sic*] HBV DNA vaccine entry into cells. PLoS One **7:**e33015. http://dx.doi.org/10.1371/journal.pone.0033015.
36. **Jung S, Unutmaz D, Wong P, Sano G, De los Santos K, Sparwasser T, Wu S, Vuthoori S, Ko K, Zavala F, Pamer EG, Littman DR, Lang RA.** 2002. *In vivo* depletion of $CD11c^+$ dendritic cells abrogates priming of $CD8^+$ T cells by exogenous cell-associated antigens. Immunity **17:**211–220. http://dx.doi.org/10.1016/S1074-7613(02)00365-5.
37. **Wu B, Zou Q, Hu Y, Wang B.** 2013. Interleukin-22 as a molecular adjuvant facilitates IL-17-producing $CD8^+$ T-cell responses to HBV DNA vaccine in mice. Hum Vaccin Immunother **9:**2133–2141.
38. **Guilliams M, Lambrecht BN, Hammad H.** 2013. Division of labor between lung dendritic cells and macrophages in the defense against pulmo-

nary infections. Mucosal Immunol **6:**464–473. http://dx.doi.org/10.1038/mi.2013.14.
39. **Othumpangat S, Noti JD, Beezhold DH.** 2014. Lung epithelial cells resist influenza A infection by inducing the expression of cytochrome c oxidase VIc which is modulated by miRNA 4276. Virology **468–470C:**256–264.
40. **Hochweller K, Striegler J, Hammerling GJ, Garbi N.** 2008. A novel CD11c.DTR transgenic mouse for depletion of dendritic cells reveals their requirement for homeostatic proliferation of natural killer cells. Eur J Immunol **38:**2776–2783. http://dx.doi.org/10.1002/eji.200838659.
41. **Wang XM, Kim HP, Song R, Choi AM.** 2006. Caveolin-1 confers anti-inflammatory effects in murine macrophages via the MKK3/p38 MAPK pathway. Am J Respir Cell Mol Biol **34:**434–442. http://dx.doi.org/10.1165/rcmb.2005-0376OC.
42. **Caspary L, Schindling B, Dundarov S, Falke D.** 1980. Infections of susceptible and resistant mouse strains with herpes simplex virus type 1 and 2. Arch Virol **65:**219–227. http://dx.doi.org/10.1007/BF01314538.
43. **Wu Y, Mao H, Ling MT, Chow KH, Ho PL, Tu W, Lau YL.** 2011. Successive influenza virus infection and *Streptococcus pneumoniae* stimulation alter human dendritic cell function. BMC Infect Dis **11:**201. http://dx.doi.org/10.1186/1471-2334-11-201.
44. **Marques CP, Cheeran MC, Palmquist JM, Hu S, Lokensgard JR.** 2008. Microglia are the major cellular source of inducible nitric oxide synthase during experimental herpes encephalitis. J Neurovirol **14:**229–238. http://dx.doi.org/10.1080/13550280802093927.
45. **Paludan SR, Malmgaard L, Ellermann-Eriksen S, Bosca L, Mogensen SC.** 2001. Interferon (IFN)-gamma and herpes simplex virus/tumor necrosis factor-alpha synergistically induce nitric oxide synthase 2 in macrophages through cooperative action of nuclear factor-kappa B and IFN regulatory factor-1. Eur Cytokine Network **12:**297–308.
46. **Welch MJ, Teijaro JR, Lewicki HA, Colonna M, Oldstone MB.** 2012. CD8 T cell defect of TNF-alpha and IL-2 in DNAM-1 deficient mice delays clearance *in vivo* of a persistent virus infection. Virology **429:**163–170. http://dx.doi.org/10.1016/j.virol.2012.04.006.
47. **Allen SJ, Mott KR, Chentoufi AA, BenMohamed L, Wechsler SL, Ballantyne CM, Ghiasi H.** 2011. CD11c controls herpes simplex virus 1 responses to limit virus replication during primary infection. J Virol **85:**9945–9955. http://dx.doi.org/10.1128/JVI.05208-11.
48. **Unkel B, Hoegner K, Clausen BE, Lewe-Schlosser P, Bodner J, Gattenloehner S, Janssen H, Seeger W, Lohmeyer J, Herold S.** 2012. Alveolar epithelial cells orchestrate DC function in murine viral pneumonia. J Clin Invest **122:**3652–3664. http://dx.doi.org/10.1172/JCI62139.
49. **Wang H, Peters N, Schwarze J.** 2006. Plasmacytoid dendritic cells limit viral replication, pulmonary inflammation, and airway hyperresponsiveness in respiratory syncytial virus infection. J Immunol **177:**6263–6270. http://dx.doi.org/10.4049/jimmunol.177.9.6263.
50. **Ryman KD, Klimstra WB, Nguyen KB, Biron CA, Johnston RE.** 2000. Alpha/beta interferon protects adult mice from fatal Sindbis virus infection and is an important determinant of cell and tissue tropism. J Virol **74:**3366–3378. http://dx.doi.org/10.1128/JVI.74.7.3366-3378.2000.
51. **Gao X, Wang S, Fan Y, Bai H, Yang J, Yang X.** 2010. $CD8^+$ DC, but not $CD8^-$ DC, isolated from BCG-infected mice reduces pathological reactions induced by mycobacterial challenge infection. PLoS One **5:**e9281. http://dx.doi.org/10.1371/journal.pone.0009281.
52. **Bruña-Romero O, Rodriguez A.** 2001. Dendritic cells can initiate protective immune responses against malaria. Infect Immun **69:**5173–5176. http://dx.doi.org/10.1128/IAI.69.8.5173-5176.2001.
53. **Hou WQ, So EY, Kim BS.** 2007. Role of dendritic cells in differential susceptibility to viral demyelinating disease. PLoS Pathog **3:**1036–1050.
54. **Tomasz M.** 1995. Mitomycin C: small, fast and deadly (but very selective). Chem Biol **2:**575–579.
55. **Trowbridge RS, Lehmann J, Torchio C, Brophy P.** 1980. Visna virus synthesized in absence of host-cell division and DNA synthesis. Microbios **29:**71–80.
56. **Sarasin A, Benoit A.** 1986. Enhanced mutagenesis of UV-irradiated simian virus 40 occurs in mitomycin C-treated host cells only at a low multiplicity of infection. Mol Cell Biol **6:**1102–1107.
57. **Terness P, Oelert T, Ehser S, Chuang JJ, Lahdou I, Kleist C, Velten F, Hammerling GJ, Arnold B, Opelz G.** 2008. Mitomycin C-treated dendritic cells inactivate autoreactive T cells: toward the development of a tolerogenic vaccine in autoimmune diseases. Proc Natl Acad Sci U S A **105:**18442–18447. http://dx.doi.org/10.1073/pnas.0807185105.
58. **Bendelja K, Vojvoda V, Aberle N, Cepin-Bogovic J, Gagro A, Mlinaric-Galinovic G, Rabatic S.** 2010. Decreased Toll-like receptor 8 expression and lower TNF-alpha synthesis in infants with acute RSV infection. Respir Res **11:**143. http://dx.doi.org/10.1186/1465-9921-11-143.
59. **Franca IL, Ribeiro AC, Aikawa NE, Saad CG, Moraes JC, Goldstein-Schainberg C, Laurindo IM, Precioso AR, Ishida MA, Sartori AM, Silva CA, Bonfa E.** 2012. TNF blockers show distinct patterns of immune response to the pandemic influenza A H1N1 vaccine in inflammatory arthritis patients. Rheumatology (Oxford) **51:**2091–2098. http://dx.doi.org/10.1093/rheumatology/kes202.
60. **Hayashi K, Hooper LC, Chin MS, Nagineni CN, Detrick B, Hooks JJ.** 2006. Herpes simplex virus 1 (HSV-1) DNA and immune complex (HSV-1-human IgG) elicit vigorous interleukin 6 release from infected corneal cells via Toll-like receptors. J Gen Virol **87:**2161–2169. http://dx.doi.org/10.1099/vir.0.81772-0.
61. **Miles DH, Thakur A, Cole N, Willcox MD.** 2007. The induction and suppression of the apoptotic response of HSV-1 in human corneal epithelial cells. Invest Ophthalmol Vis Sci **48:**789–796. http://dx.doi.org/10.1167/iovs.06-0609.
62. **Lin YL, Huang YL, Ma SH, Yeh CT, Chiou SY, Chen LK, Liao CL.** 1997. Inhibition of Japanese encephalitis virus infection by nitric oxide: antiviral effect of nitric oxide on RNA virus replication. J Virol **71:**5227–5235.
63. **Harris N, Buller RM, Karupiah G.** 1995. Gamma interferon-induced, nitric oxide-mediated inhibition of vaccinia virus replication. J Virol **69:**910–915.
64. **Murphy EA, Davis JM, Brown AS, Carmichael MD, Ghaffar A, Mayer EP.** 2008. Effect of IL-6 deficiency on susceptibility to HSV-1 respiratory infection and intrinsic macrophage antiviral resistance. J Interferon Cytokine Res **28:**589–595. http://dx.doi.org/10.1089/jir.2007.0103.
65. **Thomas BJ, Lindsay M, Dagher H, Freezer NJ, Li D, Ghildyal R, Bardin PG.** 2009. Transforming growth factor-beta enhances rhinovirus infection by diminishing early innate responses. Am J Respir Cell Mol Biol **41:**339–347. http://dx.doi.org/10.1165/rcmb.2008-0316OC.
66. **Engel S, Heger T, Mancini R, Herzog F, Kartenbeck J, Hayer A, Helenius A.** 2011. Role of endosomes in simian virus 40 entry and infection. J Virol **85:**4198–4211. http://dx.doi.org/10.1128/JVI.02179-10.